

ORIGINAL PAPER

J. T. Watson · R. E. Ritzmann

Leg kinematics and muscle activity during treadmill running in the cockroach, *Blaberus discoidalis*:

I. Slow running

Accepted: 24 May 1997

Abstract We have combined high-speed video motion analysis of leg movements with electromyogram (EMG) recordings from leg muscles in cockroaches running on a treadmill. The mesothoracic (T2) and metathoracic (T3) legs have different kinematics. While in each leg the coxa-femur (CF) joint moves in unison with the femur-tibia (FT) joint, the relative joint excursions differ between T2 and T3 legs. In T3 legs, the two joints move through approximately the same excursion. In T2 legs, the FT joint moves through a narrower range of angles than the CF joint. In spite of these differences in motion, no differences between the T2 and T3 legs were seen in timing or qualitative patterns of depressor coxa and extensor tibia activity. The average firing frequencies of slow depressor coxa (Ds) and slow extensor tibia (SETi) motor neurons are directly proportional to the average angular velocity of their joints during stance. The average Ds and SETi firing frequency appears to be modulated on a cycle-by-cycle basis to control running speed and orientation. In contrast, while the frequency variations within Ds and SETi bursts were consistent across cycles, the variations within each burst did not parallel variations in the velocity of the relevant joints.

Key words Locomotion · Electromyogram · Kinematics · Slow motor neurons · Tripod gait

Abbreviations EMG electromyogram · CF coxa-femur · FETi fast extensor tibia neuron · FT femur-tibia · T2 mesothoracic · T3 metathoracic · Ds slow depressor coxa neuron · SETi slow extensor tibia neuron · ThC thorax-coxa · Df fast depressor coxa neuron

Introduction

The contraction of muscles to produce movements provides the ultimate mechanism by which neural activity is translated into actions upon the environment, i.e., behavior. A movement is affected not only by the input of the nervous system, but also by the loading, inertia, and biomechanical properties of the body part in use. In behaviors involving the whole body, such as legged locomotion, the inertia and center of mass of the body also contribute to the movement produced by muscle contractions in any limb.

As a crucial step in understanding control of movement, investigators typically examine and characterize patterns of activity in motor neurons, either in the neurons themselves or in the resultant muscle activity. For instance, electromyographic studies of locomotion in insects have shown how the pattern of muscle activity varies with running speed (Ewing and Manning 1966; Delcomyn 1973; Krauthamer and Fourtner 1978), how the timing of muscle activity in the various legs is associated with the footfall pattern (Delcomyn 1989), and how variation in feedback from leg proprioceptors modulates motor neuron activity (Pearson 1972; Bässler 1976; Zill and Moran 1981; Cruse and Epstein 1982). In articulated phyla, contractions of limb muscles move specific joints, so the appropriate measure of muscle action is the movement of the relevant joint. The transfer function from neurophysiological data to joint movement depends upon the degree to which the movement is determined by the timing and frequency of motor neuron activity as opposed to properties of muscle and biomechanics of the limb and body. The extent to which motor activity is expressed in movements can only be assessed by a detailed analysis of the correlation between motor neuron activity and the consequent movements at specific joints.

With the recent advent of high-speed video systems, it is now possible to record even rapid movements with high resolution (Nye and Ritzmann 1992). To analyze

J.T. Watson (✉) · R.E. Ritzmann
Department of Biology, Case Western Reserve University,
Cleveland, OH 44106-7080, USA,
Tel.: +1-216 368-3591; Fax: +1-216 368-4672;
e-mail: jxw27@po.cwru.edu

the kinematics of leg movements and assess directly the relationship between motor neuron activity and movements, we have combined high-speed video recording with electromyogram (EMG) recordings from leg muscles in cockroaches running on a treadmill. Our data reveal unique joint kinematics for the middle (T2) and hind (T3) legs and consistent relationships between EMG activity and joint movements.

In systems with complex patterns of non-homogeneous motor neuron recruitment, it is extremely difficult to interpret the contribution of individual motor neuron activity to motion. The depressor coxa and extensor tibia muscles of insect legs reduce this problem, in that they are controlled by only two excitatory motor neurons (one fast and one slow type) (Usherwood 1962; Pearson and Iles 1971; Krauthamer and Fournier 1978). At slow running speeds, the slow motor neurons and their muscle fibers are used almost exclusively. During faster running or transient movements that require greater force at specific joints, the fast motor neurons are recruited (Ewing and Manning 1966; Levi and Camhi 1996). In the present paper, we focus upon the relationship between slow motor neuron activity and leg kinematics during horizontal running. In a companion paper (Watson and Ritzmann 1997) we report on changes in joint movement that occur during faster running speeds as fast motor neurons are recruited.

Our results document timing and frequency variation in motor neuron potentials as well as variation in kinematic parameters. The data suggest that motor neuron activity produces muscle forces amid complex biomechanical factors that also influence the resultant motion. A complete understanding of motor control must account for these factors. We propose a biomechanical hypothesis to account for discrepancies between variation in EMG frequency and variation in associated joint kinematics.

A preliminary report of these data has been published previously (Watson and Ritzmann 1995a).

Materials and methods

Animals

Adult male death-head cockroaches (*Blaberus discoidalis*) were used in all experiments. Cockroaches were raised in our own colony descended from 250 adult animals generously provided by Dr. Larry L. Keeley of Texas A & M University. Cockroaches were housed in 20-l plastic buckets, half-filled with aspen shavings, and were held at 27 °C in a 12-h light: 12-h dark circadian cycle. A commercial dry chicken starter and water were provided ad libitum. Only intact, undamaged cockroaches were used.

Kinematics

The ventral surface of the coxa-femur (CF) joint and the anterior surface of the tibia just distal to the femur-tibial (FT) joint were highlighted with white nail polish to facilitate visualizing them against the dark thorax of the cockroach. Each cockroach was placed individually on a motorized treadmill (manufactured by Pump and Ice Machine, Cleveland, Ohio, USA; Fig. 1A). A clear

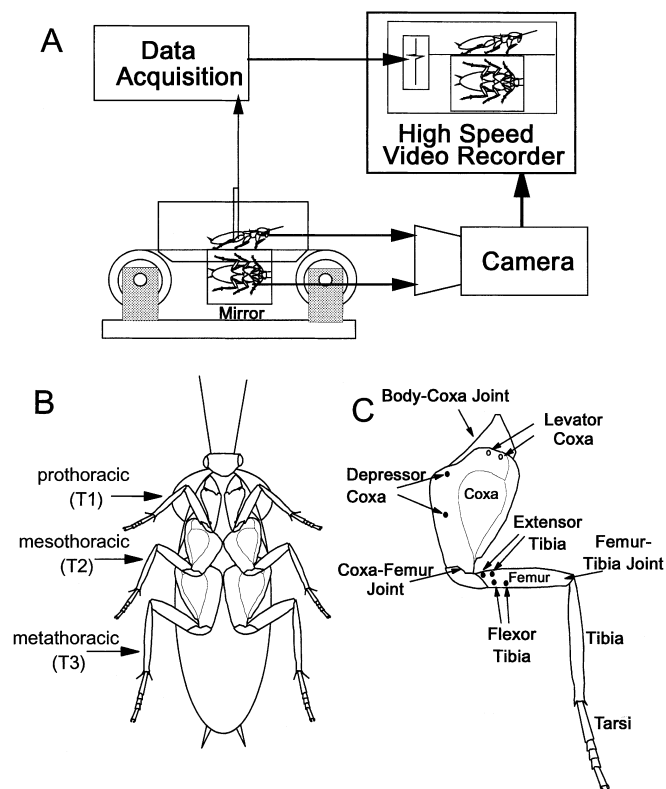


Fig. 1 **A** The experimental set-up for simultaneous electromyography and high-speed videography. **B** *Blaberus discoidalis*. **C** Leg of *B. discoidalis*, showing recording sites for recordings from depressor coxa, levator coxa, extensor tibia, and flexor tibia. The dark circles indicate recording site on the ventral surface, and the open circles indicate recording sites on the dorsal surface of the leg

acrylic chamber positioned just above the 5-cm-wide treadmill belt constrained the cockroach to run on the belt in an area of 5 cm × 17 cm. The width of the belt was approximately 1.2 times body length and 1.5 times the width of the tarsi during running, which allowed unhindered running parallel to the belt motion. The treadmill belt was clear acetate, with reference marks placed at 1-cm intervals. The lateral view of the cockroach was filmed through the acrylic chamber and the ventral view via a 7 cm × 7 cm mirror mounted at a 45° angle to the belt and immediately below it. Ventral and lateral views of the running cockroach were videotaped at 200 frames s⁻¹ with a single camera NAC HSV-400 video system. A wave inserter superimposed one EMG record onto the video image during recording.

A NAC X-Y coordinator was used to digitize joint positions. The ventral and lateral projections of the thorax-coxa (ThC), CF, FT, and tibia-tarsus joints of the leg containing EMG electrodes, as well as the anterior tip of the head and the posterior tip of the abdomen, were digitized from each video frame (Fig. 1B, C). The true CF and FT joint angles in three-dimensional space were calculated from the ventral and lateral projected images (Marx et al. 1993).

Electromyograms

Cockroaches were lightly anesthetized with CO₂ gas only while being pinned for restraint and while being released from restraint following electrode implantation for EMG recording. Cockroaches were restrained ventral side up to a cork platform with insect pins through the pronotum and insect pin staples around the trochanter and distal femur of all legs. The implantation procedure usually

lasted about 2 h, and the animal was allowed at least 1 h to recover after being released from restraint before its behavior was recorded.

Recording electrodes were 50- μ m silver wires, enamel-insulated to the tips. Pairs of wires were inserted into each muscle to a depth of < 1 mm into the muscle and glued to the overlying cuticle with cyanoacrylate cement. In each experiment, we implanted four sets of bipolar EMG electrodes and one ground wire. The multi-wire cable was glued to a minuten pin staple inserted into the lateral portion of the pronotum.

We studied the CF and the FT joints in the mesothoracic (T2) and metathoracic (T3) legs of *B. discoidalis*. In each experiment, we placed bipolar EMG electrodes in each of the following muscles of one left leg:

1. The main coxal depressor muscle 135D (T2) and 177D (T3) (Carbonell 1947) which extends the femur. It is innervated by one "slow" excitatory motor neuron (Ds) which produces slow graded contractions, one "fast" excitatory motor neuron (Df) which produces short, powerful twitches, and three inhibitors (Pearson and Iles 1971).
2. The coxal levator (138C and 182C) (Carbonell 1947) which flexes the femur and is innervated by seven motor neurons including two slow excitors (Ls), four fast excitors, and one inhibitor (Pearson and Iles 1970).
3. The tibial extensor (142a and 194a) (Dresden and Nijenhuis 1958) which is innervated by one fast excitor (FETi) and one slow excitor (SETi) (Atwood et al. 1969).
4. The tibial flexor (143 and 185) (Dresden and Nijenhuis 1958) which is innervated by nine excitors including fast, intermediate, and slow types, and two inhibitors.

The recording sites are depicted in Fig. 1C. These sites were chosen to provide the cleanest recordings of both slow and fast motor activity in the muscles that control joint movement. It should be noted that the fast and slow motor neurons to the depressor and extensor muscles recorded here also send axons to the remaining depressor and extensor muscles located in the coxa and femur leg segments. Indeed, they are the only excitatory axons to those muscles. Thus, the pattern of motor activity in these muscles should reflect the pattern of excitation to the remaining main depressor coxa and extensor tibia muscles of the leg.

EMGs were amplified 10 000 times using AC amplifiers and recorded digitally on VCR tape. In addition to the wave inserter on the video system that is described above, synchronizing the electrical and kinematic data was facilitated by recording the strobe timing pulses from the HSV recorder for each video frame (200 Hz) along with the EMGs. The onset of the timing train was gated by a stimulator that activated an LED in the HSV field of view coincident with the onset of the timing train.

Experimental protocol

Cockroaches were taken from the colony on the day before electrode implantation and pretested. Cockroaches were lightly anesthetized with CO₂, their wings were cut off, and the joints of all three left legs were marked with white nail polish. Animals were placed on the treadmill and 2–3 min of running motions were recorded using the high-speed video system. These "pretest data" were used to determine if the mechanical and physiological impact of the EMG wire implantation had any drastic effect on the leg motions during running. For each animal that was eventually used for combined kinematic and EMG analysis, three complete step cycles in the pretest condition were digitized and their kinematics analyzed. These data were also used to confirm that the differences noted below in the kinematics between T2 and T3 legs of different animals were also seen when the legs were compared within the same animal and run.

On the morning following pretests, the animals were implanted with EMG electrodes, and EMG and video data were recorded. We recorded EMGs from all four muscles in either the left T2 or left T3 leg while the cockroach ran on the motor-driven treadmill.

Data analysis

Joint angle records sampled at 200 Hz were smoothed using an even-weighted moving average of three data points each of 5 ms width. Smoothed joint angle records were expanded 50 times to give the same number of data points as the electromyograms that were digitized at a sampling rate of 10 kHz. Relevant kinematic and EMG sequences were synchronized and merged into a common file using Data-Pac software from Run Technologies. All data conditioning and subsequent analysis were also carried out with the Data-Pac systems.

Slow motor neuron potentials were discernible in the depressor coxa and extensor tibia records used for analysis. The onset and offset timing of individual EMG spikes were determined by the time when the voltage exceeded a common threshold. The threshold was set independently for each file and was chosen to maximize the number of EMG spikes detected, deflections that were clearly movement artifact or cross-talk from other muscles were edited out by hand. Slow depressor and extensor potentials were distinguished from cross-talk due to other muscles by the broad muscle potential, the relatively larger size and uniformly positive direction of the potentials, and (often) the presence of a neural spike preceding each muscle potential (see Figs. 2B, 3B for examples). Artifacts from cross-talk or extraneous noise sources was often indicated by simultaneous spikes in multiple channels (see Fig. 3B for an example). The burst onset and offset were defined as 0.5 ms before the first spike and 0.5 ms after the last spike in a burst. The mean EMG frequency was the mean of instantaneous frequencies within a burst. The mean joint angular velocity was calculated as the regression slope of the joint angle amplitude for that interval.

Because the expanded joint angle records were step functions with 5-ms steps, it was necessary to define transitions in movements in a consistent manner. The start of each joint movement was taken as 0.5 ms before the first detectable joint movement and the end was taken as 0.5 ms before the first detectable opposing movement. Two other important points in the leg cycle are the points of touchdown and liftoff of the tarsus. These points were determined directly from visual inspection of the video data, especially taking advantage of the side view, which clearly showed the point of contact and liftoff of the tarsus within the 5-ms interval of each frame.

Results

Description of data sets

Because EMGs were recorded from only one leg per animal, the data sets for T2 and T3 legs come from different animals. Comparison of leg kinematics in the same animals with and without EMG wires attached revealed that the only difference was that the excursion of the T2 CF joint was actually less in the wireless condition ($P < 0.05$). Since both the minimum and maximum joint angles were not as extreme in the pretest condition as in the EMG condition, we attributed this anomaly to sampling variability, and concluded that the EMG wires did not systematically impede leg movements.

The CF joint and FT joint kinematics and corresponding EMGs were analyzed for 56 leg joint cycles from four roaches from which EMGs had been recorded from the T2 leg and 64 joint cycles from five roaches from which EMGs had been recorded from the T3 leg. For the combined EMG-kinematic data, the median

period of the T3 joint cycles was significantly greater than the median of the T2 joint cycles examined (280.7 ms vs 183.7 ms, $P < 0.0001$). Therefore, any kinematic variables that differed between the T2 and T3 legs were confirmed by analyzing the pretest data, in which the kinematics of the two legs were recorded simultaneously from the same animal.

The movements of the leg joints during tripod running

The joint kinematics of the T2 and T3 legs have not been reported in detail before, so we describe the CF and FT joint movements to provide a basis for understanding the EMG patterns in the legs. Although the T2 and T3 legs are homologous in structure, each segmental set of legs moves in a unique way during tripod running. In the ventral projection, the T3 tibia is always seen to be parallel to the direction of body motion during stance, so the tibia is thrust rearward parallel to the coxa. In contrast, in the walking motion of the T2 leg, the tibia is oriented downward and outward with no plane parallel to the direction of motion.

During running, the ThC joints of both the T2 and T3 legs undergo motions that are small in magnitude relative to the large, planar motions of the CF and FT joints. Of its three potential degrees of freedom, the ThC joint appears to exploit one in both T2 and T3 legs and an additional one in the T2 leg in the course of each joint cycle. In both legs, the coxa twists about its long axis so that the femur is rotated upward during swing and downward to commence stance. In T2 legs the coxa also rotates perpendicular to its long axis, so the CF joint protracts during swing and retracts during stance.

Although foot set-down occurred at the same phase of the CF joint cycle in T2 and T3, the phase of the CF joint cycle at which CF extension started was significantly earlier in T2. Thus, on average, the T2 CF joint began to extend one or two video frames (mean = 6 ± 1.1 ms) after the tarsus contacted the treadmill, so the tarsus was actually moving forward relative to the treadmill when it first made contact. In T3 legs, the CF joint began to extend either one frame before foot set-down or in the same frame as foot set-down (mean = 2 ± 1.7 ms, $P < 0.01$, Mann-Whitney Rank-Sum Test). Thus, the CF joint often began extending while the tarsus was still in the air, so that the tarsus was already moving rearwards relative to the animal when it contacted the treadmill. Our kinematics make an interesting comparison with the ground reaction forces measured for each set of legs (Full et al. 1991). The horizontal ground reaction force produced by the T3 legs is exclusively accelerating, while the T2 leg produces initially braking, then accelerating horizontal ground reaction forces. Our observations that the tarsus sets down before the CF joint begins extending in T2 legs and the CF joint begins extending before the tarsus sets down in T3 legs are consistent with the reported patterns of horizontal ground reaction forces.

The relationship of the CF joint to the FT joint during tripod running

Figure 2 shows the CF and FT joint angles of the T2 leg synchronized with EMG records during tripod walking. Figure 3 shows comparable data in another animal for T3 legs. In both legs, the CF and FT joints extend during stance and flex during swing. In the T3 leg, the trajectory of the tibia requires that the CF and the FT joints move in parallel and their excursions are not significantly different. The CF joint angle was highly correlated with the FT joint angle in the T3 legs ($R = 0.88$, $P < 0.0001$). The CF joint angle was not as highly correlated with the FT joint angle in the T2 legs ($R = 0.514$, $P < 0.0001$). This lower correlation is due to the complex motion of the T2 leg, and is reflected differences in joint excursion. The T2 FT joint undergoes slightly more than one-half the excursion of the T2 CF joint (mean CF excursion = 43.9° , mean FT excursion = 26.0° ; $P < 0.0001$). In contrast, the CF and FT joints in the T3 legs undergo approximately the same excursion (mean CF excursion = 53.9° , mean FT excursion = 52.2° ; $P = 0.26$).

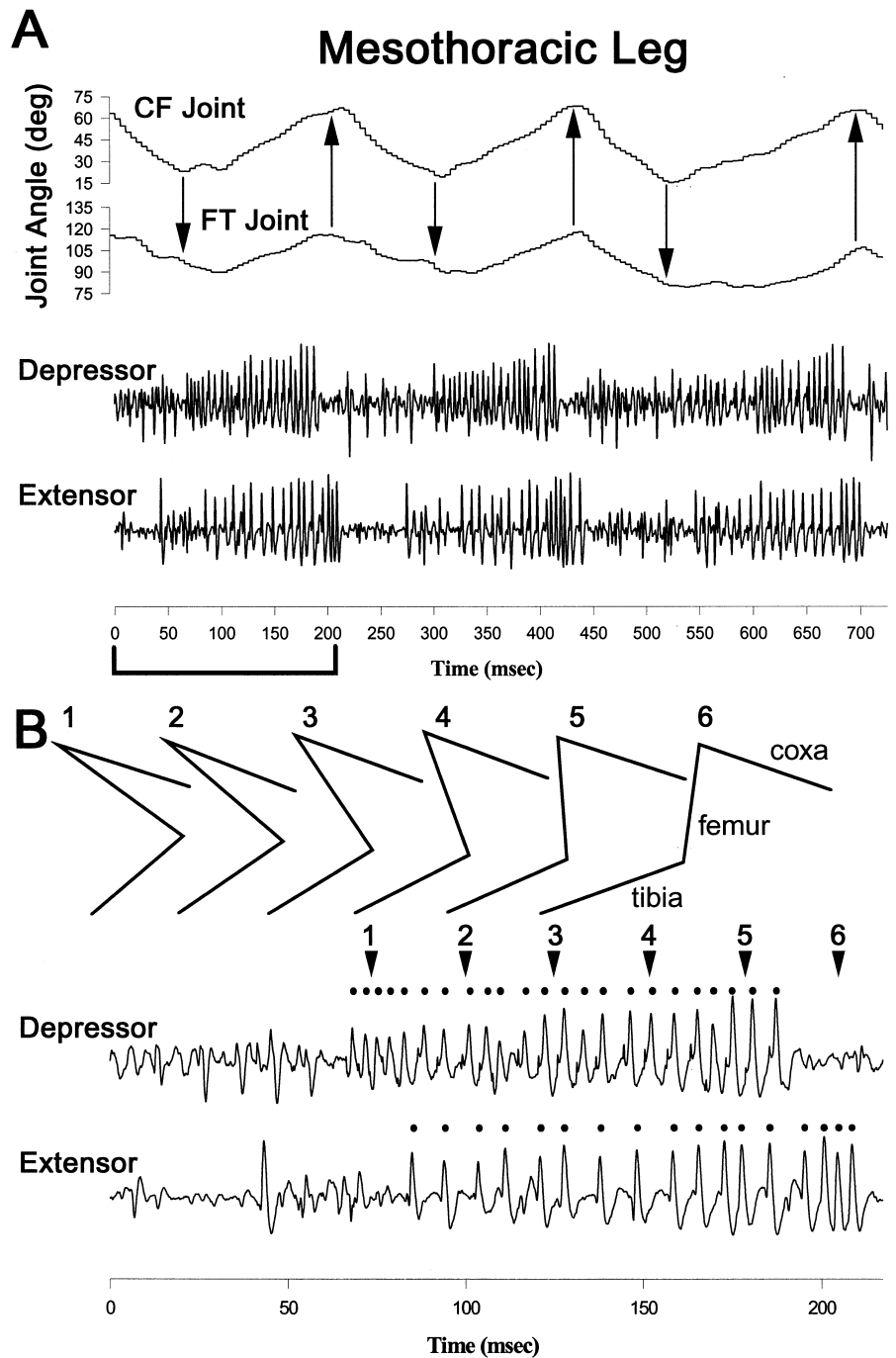
In both legs, CF joint extension typically preceded FT joint extension during each joint cycle and there was no difference between the legs in the CF extension to FT extension delay (onset delay: T2: 11 ± 1.4 ms, T3: 15.4 ± 1.7 ms; and offset: T2: 3.6 ± 0.9 ms, T3: 8.2 ± 1.4 ms; differences between T2 and T3 not significant by Mann-Whitney test).

Relationship of slow motor neuron frequency to joint angular velocity

Frequency of motor activity is typically considered to be one of the prime determinants for controlling muscle contraction, and consequently velocity of joint movement. We compared the mean frequency of Ds and SETi muscle potentials with mean joint angular velocity for those joint cycles in which only slow motor neurons were active (2–5 Hz). For each joint examined, the average firing frequency of the slow depressor or extensor motor neuron was directly proportional to the average angular velocity of the relevant joint during extension (Fig. 4).

As shown above, the kinematic relationship between the CF and FT joints differed between the two legs. This was reflected in the relationships between EMG frequency and joint angular velocity. The T2 FT joint operated in a lower velocity range than the other joints because it traversed about half the excursion over the same time frame. In addition to this difference in velocity, the relationship between EMG frequency and joint angular velocity was unique for the T2 FT joint. The EMG frequency versus joint angular velocity functions for both T3 joints as well as the T2 CF joint were virtually overlapping (Fig. 4). In contrast, the slope of the SETi frequency versus FT angular velocity function for the T2 leg was lower than that for the same

Fig. 2 A CF and FT joint angle records synchronized with depressor coxa and extensor tibia EMG records from the mesothoracic leg of a cockroach running at 4–5 Hz on a treadmill. Superimposed on the motion records, the *downward arrows* indicate the points at which the tarsus contacted the treadmill and the *upward arrows* indicate the points at which the tarsus lifted from the treadmill. **B** Expansion of the EMGs from the first step in A (as indicated by the *bar* under that portion of the record). *Stick figures*, taken directly from digitized video data, depict the ventral projection of the leg to show the details of motion during one extension. The *numbered arrows* indicate the points in time corresponding to each stick figure. The first step is on the extreme left and the sequence proceeds to the right. Each stick figure was displaced laterally to aid in visualizing each joint. *Dots* have been placed above each muscle potential attributed to either the slow coxal depressor or slow extensor tibia in the respective EMG records. Criteria for distinguishing the slow depressor and extensor potentials from cross-talk and other artifacts are described in the text



function in the T3 leg ($P < 0.05$, t -test). Thus, comparable changes in EMG frequency are associated with less of an increase in joint angular velocity at the FT joint of the T2 leg than in the FT joint of the T3 leg.

Modification of EMG frequency during turning

If the CNS controls joint angular velocity by varying the firing frequency of motor neurons, then variations in EMG frequency should be apparent not only in relation to variations in running speed, but also when legs are

moved at different speeds relative to one another. For example, the animal can execute a turn while running forward by increasing the velocity of joint extension in the stance leg on one side while decreasing joint extension velocity in the stance leg on the other side. This should be accompanied by appropriate dissociations of mean Ds and SETi discharge rate from overall stepping speed.

The turning behavior exhibited by *B. discoidalis* while running forward within the confines of the experimental treadmill setup consisted of alterations in body orientation by 15–30°. Such changes in body orientation took

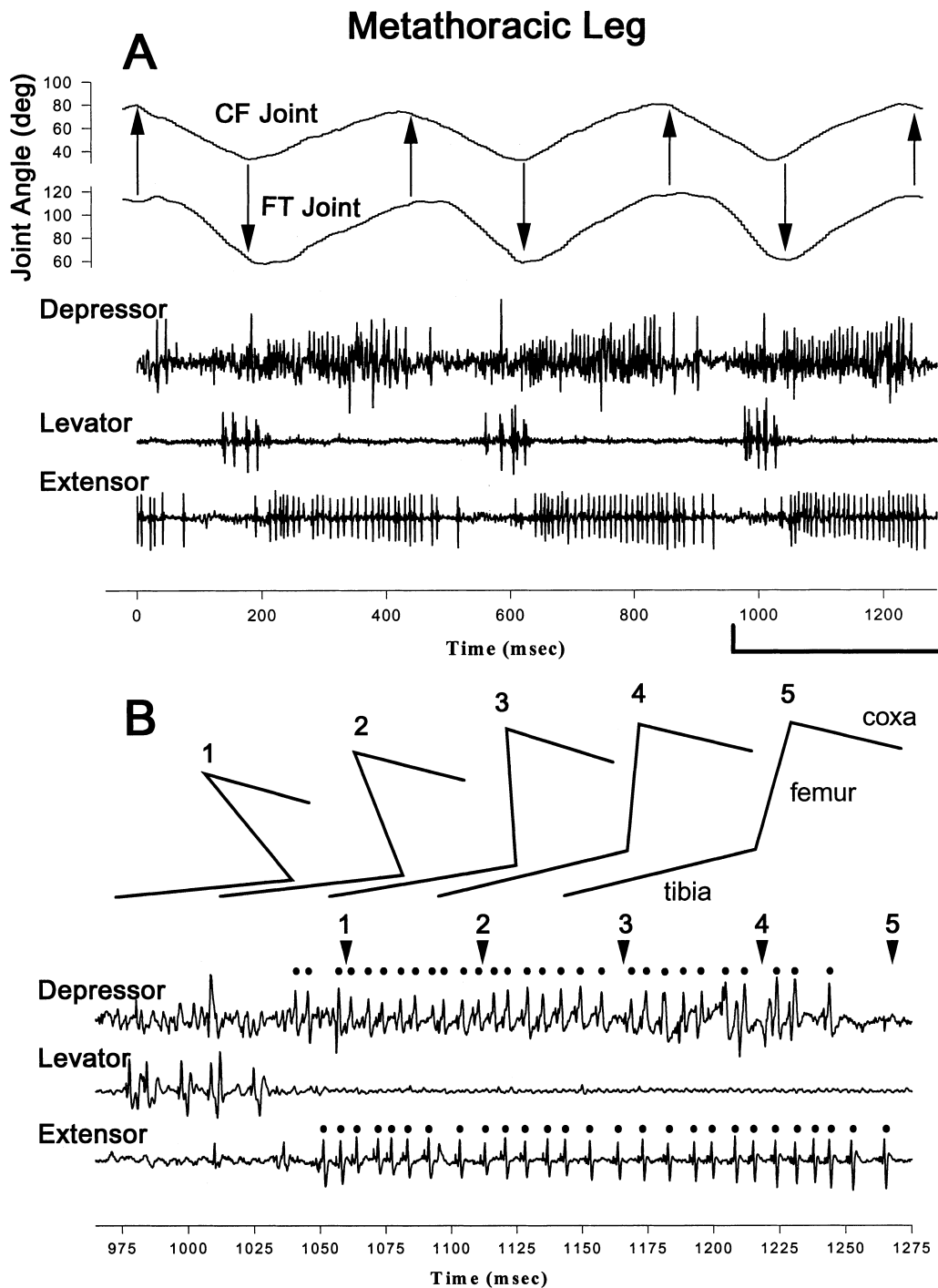


Fig. 3A CF and FT joint angle records synchronized with depressor coxa, levator coxa, and extensor tibia EMG records from the metathoracic leg of a cockroach running at 2–2.5 Hz treadmill. Superimposed on the motion records, *arrows* indicate tarsal touch-down and liftoff, as in Fig. 2. **B** Expansion of the EMGs from the third step in A (as indicated by the *bar* under that portion of the record). *Stick figures* of the leg show the details of motion during one extension. Note the greater FT excursion evident in this set of stick figures in comparison with those for T2 legs in Fig. 2. The slow coxal depressor and slow tibial extensor motor neuron potentials have been identified, as in Fig. 2. Even though the start point of each Ds burst is not obvious in A, when the record was spread out as in B, the appropriate potentials are clearly distinguished from crosstalk and artifacts, such as the one seen in all three channels at 1100 ms. In all of our analysis, we inspected the computer records visually in this manner to verify correct positioning of events

place during the stance phase of one tripod set of legs (two sequential turns are shown in Fig. 5A). Within our data set, there were seven right turns and six left turns. Because the EMG electrodes were always in a left leg (either T2 or T3), right turns allowed us to correlate EMG activity with joint velocity in a leg that was on the outside of the turn while left turns allowed us to look at the same function in a leg on the inside of the turn. For T2 legs, the turn data are consistent with the data from straight running, but the EMG frequency and joint angular velocity for turns are clustered in the low range when the turn is toward the leg and in the high range when the turn is away from the leg (Fig. 5B). Right turns

Fig. 4A, B The mean velocity of joint extension is linearly related to the mean rate of firing of the slow motor neuron at each joint. Average slow depressor coxa and slow extensor tibia EMG frequency versus average joint angular velocity for the CF and FT joints of **A** the mesothoracic leg (T2) and **B** the metathoracic leg (T3) during straight running. Data are from cycles with only slow motor neuron activity

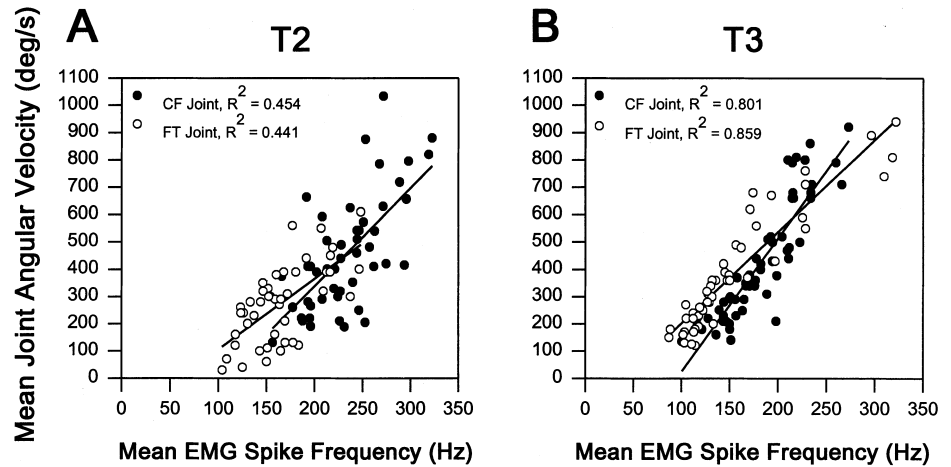
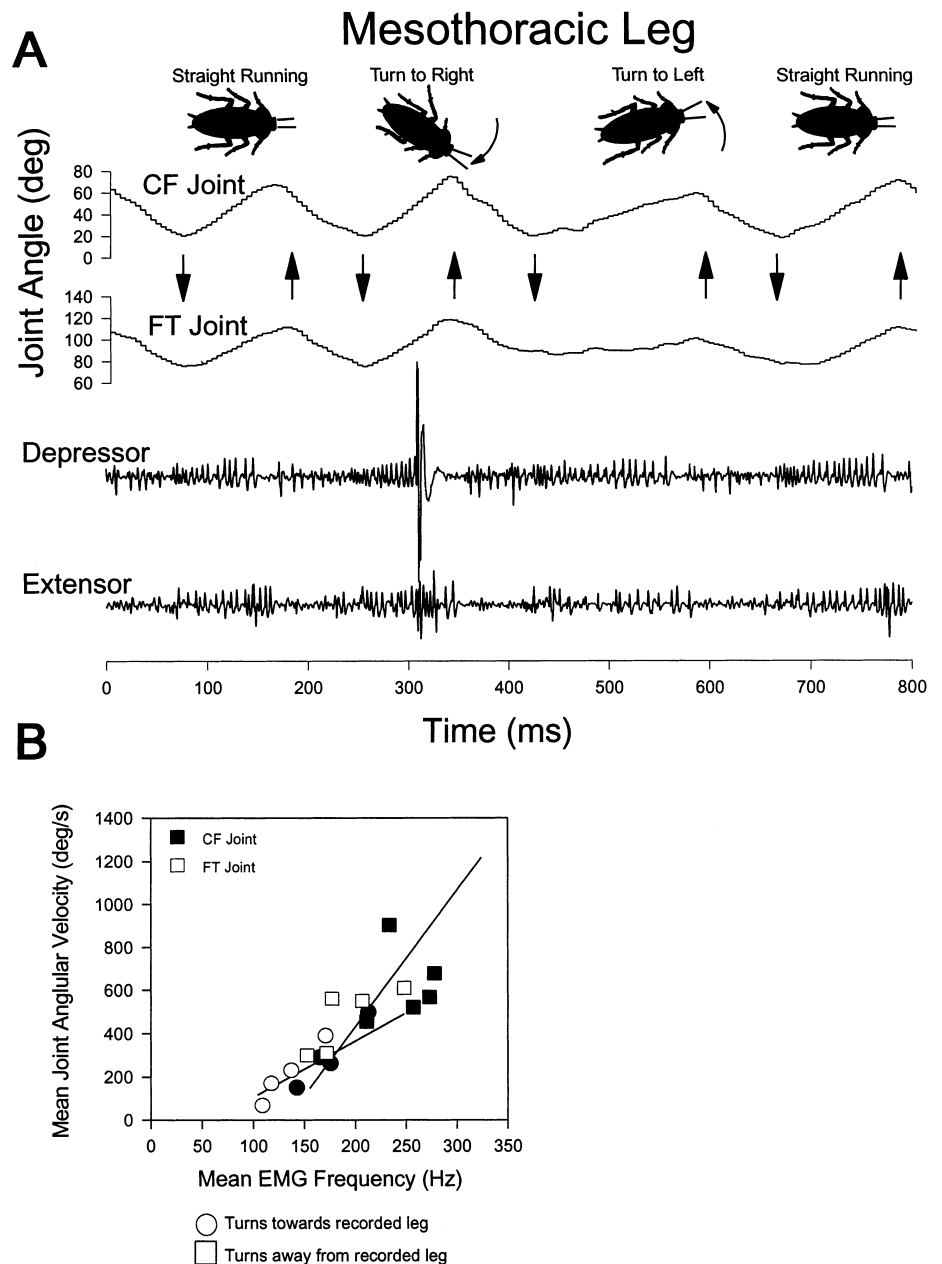


Fig. 5A, B Turns during tripod running are executed by increasing depressor and extensor activity on one side of the animal while decreasing it on the other side. **A** CF and FT joint angle records synchronized with depressor coxa and extensor tibia EMG records, from the left mesothoracic leg (T2) of a cockroach. This animal executed a right turn while the left T2 tarsus was on the ground in the second step and a left turn while left T2 tarsus was on the ground in the third step. **B** Mean slow motor neuron frequency versus mean joint extension velocity from the mesothoracic (T2) leg during steps when the animal was turning. The lines are the regressions for all the running data as in Fig. 4. The circles indicate data from left turns (towards the recorded leg) and the squares indicate data from right turns (away from the recorded leg). Note that the points for turns away from the recorded leg are clustered at higher EMG frequencies, whereas for turns towards the recorded leg they are clustered at lower EMG frequencies



involved a significant increase in T2 depressor and extensor activity and significantly higher mean CF and FT joint angular velocities relative to the straight running steps immediately preceding and following the turn ($P < 0.05$; paired t -test). Left turns in T2 legs involved a significant decrease in depressor and extensor activity and an associated decrease in joint velocity in the leg relative to straight running ($P < 0.05$; paired t -test). For T3 legs the data were not as clearly clustered at the extremes. This may be a real difference from T2 legs or may be a result of the fact that we recorded muscle activities in T3 legs during a smaller number of turns.

Analysis of EMG activity within joint cycles

Within each joint flexion-extension cycle the EMG bursts are not homogeneous; rather, there are consistent frequency patterns for the Ds and SETi motor neurons.

Timing of motor activity

Cumulative frequency histograms of joint cycles ranging from 2 Hz to 5 Hz, that contain only slow motor activity, are shown in Fig. 6. For both legs, Ds and SETi showed a large increase in activity between phase 35% and 40%, and a large decrease in activity near phase 90% of the joint cycle. Activity in the levator coxa motor neurons was confined to the period of CF flexion, whereas activity in the flexor tibia motor neurons persisted into the early phase of FT extension, in a highly variable period of co-contraction with SETi.

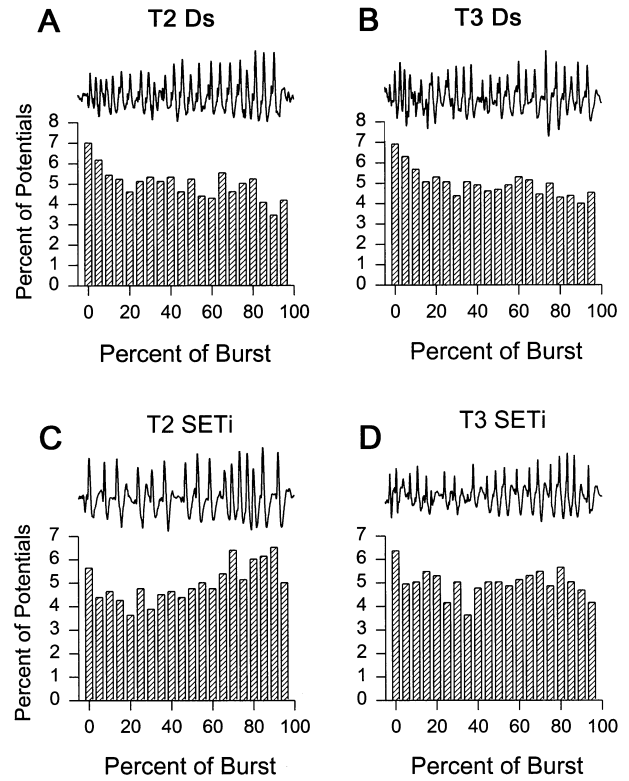
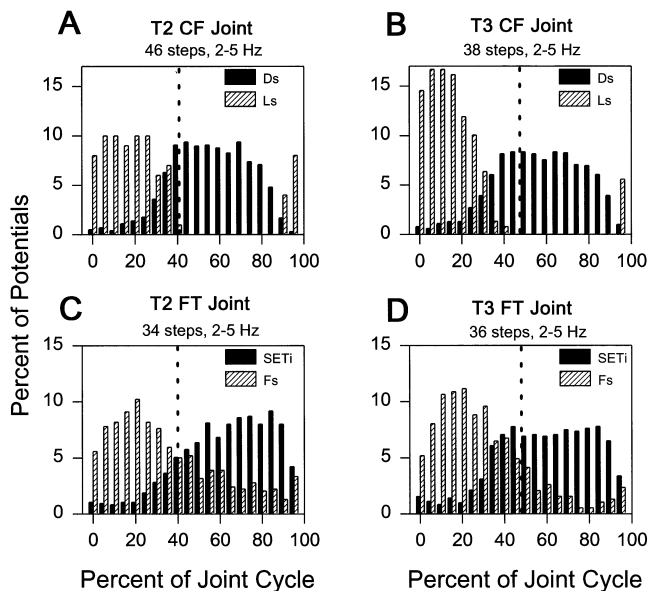


Fig. 7A–D High-frequency intervals occur consistently within each Ds and SETi burst. EMG activity, normalized to burst duration, from joint cycles in which only slow motor neurons were active (2–5 Hz running speed, 15 cycles are summarized in each histogram). Above each histogram is a single EMG burst to illustrate the sort of data from which the histograms were derived. **A** Mesothoracic (T2) leg Ds. **B** Metathoracic (T3) leg Ds. **C** T2 SETi. **D** T3 SETi

Patterns of muscle potential frequency within bursts

In both T2 and T3 legs, there was a consistent pattern of EMG frequency variation within Ds and SETi bursts which is not apparent in Fig. 6. Figure 7 shows histograms of muscle potentials normalized across bursts for Ds and SETi in both legs along with representative samples of raw data. Several features are apparent from these data.

The Ds pattern in both legs includes a high-frequency period during the first 10% of the burst. This period commences and ends as the joints move through reasonably consistent angles. The onset of Ds activity starts at $20.3 \pm 6^\circ$ (mean \pm SD) in T2 and $29.6 \pm 9^\circ$ in T3 legs. The joints then flex to smaller angles and, as they

Fig. 6A–D EMG activity from joint cycles in which only slow motor neurons were active, normalized to joint cycle duration. The number of joint cycles is indicated above each histogram. **Filled bars**: Ds and SETi; **cross-hatched bars**: slow levator (Ls) and slow flexor (Fs). **A** Mesothoracic (T2) leg CF joint. **B** Metathoracic (T3) leg CF joint. **C** T2 FT joint. **D** T3 FT joint. For these plots, the joint cycle starts at the extension to flexion transition and the *vertical dashed line* indicates the flexion to extension transition

extend, the high-frequency period stops at $24.3 \pm 5^\circ$ in T2 and $31.6 \pm 7^\circ$ in T3 legs. In both legs SETi has a much briefer initial high-frequency period, and SETi typically increases in frequency toward the end of the burst. Interestingly, the early high-frequency periods in Ds and late high-frequency period in SETi coincide with the point at which the respective fast motor neurons for these joints are recruited as the animal runs faster (Watson and Ritzmann 1997).

Relationship of motor neuron intraburst patterns to joint angular velocity

Given the positive correlations between mean joint angular velocity and mean motor neuron frequency, one might expect that the high-frequency periods at the beginning of Ds bursts and the end of SETi bursts would be reflected in increased joint velocity during those periods. To test this notion, we divided the bursts into three regions: the first five EMG spikes, the middle five spikes and the last five spikes in each burst and performed regression analyses between mean muscle potential frequency and mean joint angular velocity for each interval (Table 1). For Ds and SETi in T2 legs and for SETi in T3 legs, the highest correlation between EMG frequency and joint angular velocity was found for the middle segment. Ds in T3 legs showed poor correlations for all three segments but slightly better for the middle and last segments. Thus, the high-frequency components seen early in Ds bursts and early and late in SETi bursts were less correlated with joint angular velocity than EMG activity in the middle of each burst. This finding may be related to the fact that these segments occur during transitions between flexion and extension; this point is discussed in Watson and Ritzmann (1997).

Discussion

By combining high-speed video analysis with electrophysiology, we were able to relate kinematics of specific joint movements during free-running behavior with the motor activity that excites the appropriate muscles and ultimately causes joint movement. Our data are consistent with the notion that an animal's central nervous system controls the velocity of joint movement by modifying motor neuron frequency. This observation is, of course, not surprising. However, motor neuron activity is read out in the context of complex biomechanical factors that influence the resultant motion. The biomechanics of each leg determine the exact relationship between motor neuron frequency and movement for each joint. Because the morphology of each segmental pair of legs and the forces they generate are unique (Full et al. 1991), the transfer functions for motor neuron activity to motion are also leg and joint specific. In addition, variations in frequency within EMG bursts are not consistently reflected in kinematic variations within each joint cycle.

The mean frequencies of Ds and SETi potentials are linearly related to the mean velocities of respective joint extension movements during stance. The correlation was found for both Ds and SETi in both the T2 and T3 legs, and was consistent with a previous report of depressor EMG frequency correlating with step-cycle duration (Delcomyn 1971). This result was consistent with the model of Pearson and Iles (1970), which proposes that the frequency of a continuous central command circuit sets the extensor discharge period, burst duration and discharge rate.

The linear relationship between mean motor neuron activity and mean joint velocity clearly indicates that motor activity can be altered to increase joint velocity in a coordinated manner in all joints when faster running

Table 1 Regressions of EMG mean frequency versus corresponding mean joint angular velocity

	<i>n</i>	<i>R</i>	<i>R</i> ²	<i>P</i>
T2 leg				
Entire Ds burst vs entire CF extension	61	0.674	0.454	<0.0001
Entire SETi burst vs entire FT extension	39	0.664	0.441	<0.0001
First 5 Ds potentials vs first 5 CF intervals	36	0.487	0.237	0.117
Middle 5 Ds potentials vs middle 5 CF intervals		0.653	0.410	<0.0001
Last 5 Ds potentials vs last 5 CF intervals		0.447	0.176	0.0063
First 5 SETi potentials vs first 5 FT intervals	33	0.235	0.025	0.1874
Middle 5 SETi potentials vs middle 5 FT intervals		0.722	0.506	<0.0001
Last 5 SETi potentials vs last 5 FT intervals		0.288	0.053	0.1046
T3 Leg				
Entire Ds burst vs entire CF extension	54	0.895	0.801	<0.0001
Entire SETi burst vs entire FT extension	43	0.927	0.859	<0.0001
First 5 Ds potentials vs first 5 CF intervals	33	0.487	0.213	0.040
Middle 5 Ds potentials vs middle 5 CF intervals		0.611	0.353	0.0002
Last 5 Ds potentials vs last 5 CF intervals		0.611	0.353	0.0002
First 5 SETi potentials vs first 5 FT intervals	32	0.521	0.248	0.0022
Middle 5 SETi potentials vs middle 5 FT intervals		0.789	0.609	<0.0001
Last 5 SETi potentials vs last 5 FT intervals		0.408	0.138	0.0227

speeds are desired. The changes in mean firing rate and joint velocity at individual joints during turns indicate that the CNS also uses this relationship to control orientation. During tripod running, the animal determines its orientation by adjusting the frequency of depressor and extensor motor neuron activity to control the relative force output on opposite sides of the body. Depending upon which T2 leg is in contact with the ground, the animal either increases firing rate in the depressor and extensor motor neurons creating a turn away from the leg or decreases the firing rate creating a turn toward the leg. This modulation appears to be controlled on a step-by-step basis to effect either straight running or turning.

A mechanism by which the insect nervous system could control the mean firing frequency of motor neurons has been known since the early studies by Pearson and Fourtner (1975). Non-spiking interneurons can directly drive activities of motor neurons to leg muscles. Changes in membrane potential in non-spiking interneurons have been shown to produce graded changes in the membrane potential and firing frequencies of slow motor neurons (Burrows and Siegler 1978; Burrows 1980). The linear relationship between the membrane potential of non-spiking interneurons and postsynaptic voltage in slow motor neurons indicates that these interneurons can effectively set the mean firing rate of motor neurons. Input drive from non-spiking interneurons could be the mechanism which sets the frequency of motor neuron firing, which our data indicate determine the rate of joint extension during walking.

Even though mean frequency is reflected in the kinematics of joint motion, it is not the complete story. The biomechanics of the joints are also important and vary between each pair of legs. As is clear from studies on ground reaction forces (Full et al. 1991), the role played by each pair of legs is unique. The T2 and T3 legs produce markedly different lateral and horizontal ground reaction forces. The horizontal ground reaction force produced by the T3 legs is exclusively accelerating, while the T2 leg produces initially braking, then accelerating horizontal ground reaction forces. The T2 leg produces 1.6 times higher lateral ground reaction force than the T3 leg. Our data revealed that the kinematics and the relationships between EMG frequency and joint angular velocity were similar for the T2 CF joint and the T3 CF and FT joints, while the T2 FT was different. While in T3 legs the FT and CF joints extend in parallel so the tibia is thrust rearward parallel to the coxa, in T2 legs the tibia is oriented more laterally while moving rearward, and the FT joint undergoes less excursion than the CF joint. Thus, the high lateral ground reaction force characteristic of the T2 leg is produced with about half the FT excursion of the T3 leg. The more limited extension of the T2 FT joint at high SETi frequencies suggests that, due to imposed torque on this joint during fast running, it is doing more negative work than the T3 FT joint. Although our data are in general consistent with the data reported by Full et al. (1991), it should be

noted that their data were typically taken from animals running at much faster speeds.

The complexity of the transfer function is further indicated by the comparisons of motor activity to joint movement within individual joint cycles, where characteristic features of motor neuron bursts were not always correlated with joint kinematics. The kinematic records did not show inflections in joint angle movement corresponding to changes in EMG frequency. The relatively weak correlation between instantaneous EMG frequency and joint angular velocity contrasts with studies in which motor neurons were stimulated while monitoring the movements of unloaded legs (Usherwood 1962; Watson and Ritzmann 1995). Those studies did show precise relationships between individual EMG potentials and movement.

Two explanations for the lack of correlation in intraburst features during free running are possible. First, the intraburst features could be an epiphenomenon of the central pattern-generation circuitry and the insect neuromuscular system. The details of frequency modulations in motor neuron bursts could be filtered by the cumulative effects of biomechanical efficiency of the muscles and joints, viscous forces within the leg, and whole body inertia so as to have no direct relationship to the details of joint movements. Alternatively, it is possible that the frequency modulation within bursts represents proprioceptive reflexes, which tune the motor output to events that occur consistently at particular points in each joint cycle. In this scenario, the nervous system uses proprioceptive reflexes to generate the intraburst features which actually eliminate inflections and result in the smooth fluid movements that are characteristic of animal locomotion. Our data, taken with those of other reports, are in general inconsistent with the passive filtering hypothesis, and consistent with the hypothesis that tuning of motor output overcomes load variations within the joint cycle.

There are three types of evidence that address these hypotheses. First, the timing of the highest-frequency activity within Ds and SETi bursts is associated with particular parts of the step cycle. The sequence of events during each joint cycle is as follows (Fig. 8). Ds begins firing at a high frequency during flexion of the CF and FT joints, *before* the tarsus touches down. The high frequency Ds activity begins and ends at specific joint angles and spans the flexion to extension transition. In both legs, the joint angle at which the high-frequency Ds burst begins during flexion is correlated with the joint angle at which Ds frequency decreases during extension. SETi activity commences shortly after Ds initiation and right before the FT joint begins its extension. The tarsus touches down on the substrate at or near the transition from flexion to extension of the CF joint. It then lifts off the substrate slightly after the transition from extension to flexion. Both the fast depressor and fast extensor motor neurons are recruited at the same time as the highest frequency appears in the respective slow motor neurons (Watson and Ritzmann 1997). This coincidence

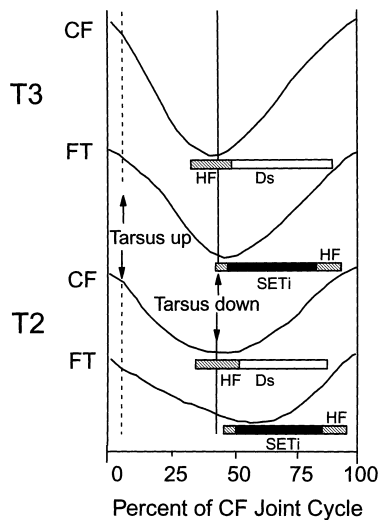


Fig. 8 Summary of timing of CF and FT joint movements and associated Ds and SETi activity. The joint angle records are averages of 15 cycles of the two principal joints of the T2 and T3 legs, selected so as to match joint cycle period. The phase of the tarsal set down, and motor neuron burst onsets and offsets were the means from the analyzed steps. The shaded areas on the EMG bars, marked HF indicate the timing of the high-frequency components of EMG bursts. All traces are presented relative to the initiation of CF flexion of each leg

suggests that these points in the joint cycle require extra force, and fast motor neurons are recruited to modulate muscle force more rapidly at these times. Indeed, all of the EMG features described above occur with very precise timing within the joint cycle. The precision of their timing suggests that they are important features that are not filtered out by the mechanics of muscle.

Second, there is evidence that altering proprioceptive input affects intraburst patterning. There is a wealth of proprioceptive structures associated with each leg, and the timing of some of the intraburst features is consistent with activation of particular sensory structures. For example, the beginning and ending of the high-frequency burst in Ds are highly correlated with specific joint angles in each leg. The timing of this event may be linked to the transition from flexion to extension or to the increased loading that will occur when the foot touches down on the substrate. Reflex activation of extensor motor neurons by the proximal tibial campaniform sensilla has been demonstrated in *Periplaneta americana* (Zill and Moran 1981a, b; Zill et al. 1981). In animals with one leg amputated at the distal femur, so that the trochanteral campaniform sensilla are not loaded during walking, the timing of SETi bursts is normal but the intraburst structure characteristic of normal walking is absent (Zill et al. 1995). Moreover, during inverted walking, the extensor activity in the first half of stance phase is replaced by flexor activity which contributes to supporting the inverted animal against gravity (Duch and Pflüger 1995; Larsen et al. 1995).

Third, the timing of intraburst features relative to joint movement that we describe here is not unique to insects. For example, bursts of EMG activity occur in

the stance-related lateral gastrocnemius and the vastus lateralis muscles of the cat hind limb preceding foot set-down during walking (Gorassini et al. 1994). This suggests that the timing and frequency patterning of extensor bursts is a function of the requirements of legged locomotion, rather than an epiphenomenon of insect thoracic circuitry.

At the flexion-extension transition, loading suddenly increases as the tarsus touches down, the extensor muscles may be at a mechanical disadvantage at extremely flexed joint angles, and there may be extensive co-contraction of extensors and flexors to stiffen joints for the onset of stance. Unfortunately, the only data currently available on cockroach running, namely EMG recordings of muscle activity, force plate recordings of ground reaction forces, and kinematic analysis of movements do not resolve the joint stiffnesses, torques about joints and muscle loads which the cockroach leg experiences at this transition. For example, the ground reaction force produced by each leg during running does not peak at the onset of stance, but reaches its maximum at mid-stance (Full et al. 1991). Co-activation of antagonist muscles may serve to stiffen a joint. Co-activation at the flexion-extension transition of the muscles that control the FT joint has been observed in a number of species of cockroach (Ewing and Manning 1966; Krauthamer and Fourtnier 1978; Larsen et al. 1995), and was seen in many of our recordings. However, at the flexion-extension transition, we did not observe co-activation of depressor and levator coxa muscles that control CF joint movement. Given the complexity of the levator coxa and flexor tibia motor neuron populations in the cockroach leg, it is always difficult to be sure that all levator or flexor activity is accounted for in EMG recordings, and to eliminate the possibility that co-activation is occurring.

Nevertheless, our detailed analyses of the correlation between depressor and extensor motor neuron activity and the consequent movements at specific joints reveal the extent to which that activity is expressed in movements during running. The Ds and SETi firing frequencies are correlated on a cycle-by-cycle basis with CF and FT joint angular velocities, suggesting that these variables are actively modulated by the central pattern generator to control running speed and orientation. The function relating motor neuron frequency to joint angular velocity is markedly different in the T2 FT joint, reflecting different biomechanics for this joint. In contrast, while the frequency variations within Ds and SETi bursts were consistent across cycles, the frequency variations within each burst did not parallel variations in the velocity of the relevant joint. Our data are consistent with other studies on proprioceptive feedback which suggest that intraburst properties are tuned to compensate for biomechanical loading discontinuities and result in smooth fluid movements.

Acknowledgements We wish to thank two anonymous reviewers for insightful suggestions on the discussion and presentation of the

data, Robert J. Full for helpful discussions and sharing data relevant to this manuscript, Mr. and Mrs. James A. Lafer for extensive technical assistance, and the Cadillac Corporation for the generous donation of video analysis equipment. This research was supported by ONR grant N00014-90-J-1545.

References

- Atwood HL, Smyth T, Johnston HS (1969) Neuromuscular synapses in the cockroach extensor tibia muscle. *J Insect Physiol* 15: 529–535
- Bässler U (1976) Reversal of a reflex to a single motoneuron in the insect *Carausius morosus*. *Biol Cybern* 24: 47–49
- Burrows M (1980) The control of sets of motoneurons by local interneurons in the locust. *J Physiol (Lond)* 298: 213–233
- Burrows M, Siegler VMS (1978) Graded synaptic transmission between local interneurons and motor neurones in the meta-thoracic ganglion of the locust. *J Physiol (Lond)* 285: 231–255
- Carbonell CS (1947) The thoracic muscles of the cockroach *Periplaneta americana* (L.). *Smithson Misc Collect* 107: 1–23
- Cruse H, Epstein S (1982) Peripheral influences on the movement of the legs in a walking insect *Carausius morosus*. *J Exp Biol* 101: 161–170
- Delcomyn F (1971) The locomotion of the cockroach *Periplaneta americana*. *J Exp Biol* 54: 443–452
- Delcomyn F (1973) Motor activity during walking in the cockroach *Periplaneta americana*. I. Free walking. *J Exp Biol* 59: 629–642
- Delcomyn F (1989) Walking in the American cockroach: the timing of motor activity in the legs during straight walking. *Biol Cybern* 60: 373–384
- Dresden D, Nijenhuis ED (1958) Fiber analysis of the nerves of the second thoracic leg in *Periplaneta americana*. *Proc K Ned Akad Wetser C* 61: 213–233
- Duch C, Pflüger HJ (1995) Motor patterns for horizontal and upside-down walking and vertical climbing in the locust. *J Exp Biol* 198: 1963–1976
- Ewing AW, Manning A (1966) Some aspects of the efferent control of walking in three cockroach species. *J Insect Physiol* 12: 1115–1118
- Full RJ, Blickhan R, Ting LH (1991) Leg design in hexapedal runners. *J Exp Biol* 158: 369–390
- Gorassini MA, Prochazka A, Hiebert GW, Gauthier MJ (1994) Corrective responses to loss of ground control during walking. I. Intact cats. *J Neurophysiol* 71: 603–610
- Krauthamer V, Fourtner CR (1978) Locomotory activity in the extensor and flexor tibiae of the cockroach, *Periplaneta americana*. *J Insect Physiol* 24: 813–819
- Larsen GS, Frazier SF, Fish SE, Zill SN (1995) Effects of load inversion in cockroach walking. *J Comp Physiol A* 176: 229–238
- Levi R, Camhi JM (1996) Producing directed behaviour: muscle activity patterns of the cockroach escape response. *J Exp Biol* 199: 563–568
- Marx WJ, Beer RD, Nelson G, Quinn R, Crocker GA (1993) A biomechanical model of the cockroach leg. *Soc Neurosci Abstr* 19: 1601
- Nye SW, Ritzmann RE (1992) Motion analysis of leg joints associated with escape turns of the cockroach, *Periplaneta americana*. *J Comp Physiol A* 171: 183–194
- Pearson KG (1972) Central programming and reflex control of walking in the cockroach. *J Exp Biol* 56: 173–193
- Pearson KG, Fourtner CR (1975) Nonspiking interneurons in walking system of cockroach. *J Neurophysiol* 38: 33–52
- Pearson KG, Iles JF (1970) Discharge patterns of coxal levator and depressor motoneurons of the cockroach, *Periplaneta americana*. *J Exp Biol* 52: 139–165
- Pearson KG, Iles IF (1971) Innervation of coxal depressor muscle in the cockroach, *Periplaneta americana*. *J Exp Biol* 54: 215–232
- Usherwood PNR (1962) The nature of 'slow' and 'fast' contractions in the coxal muscles of the cockroach. *J Insect Physiol* 8: 31–52
- Watson JT, Ritzmann RE (1995a) Combined intracellular stimulation and high speed video motion analysis of motor control neurons in the cockroach. *J Neurosci Methods* 61: 151–157
- Watson JT, Ritzmann RE (1995b) Kinematic and EMG analysis of locomotion in the cockroach. *Soc Neurosci Abstr* 21: 427
- Watson JT, Ritzmann RE (1997) Leg kinematics and muscle activity during treadmill running in the cockroach, *Blaberus discoidalis*. II. Transition to fast running. *J Comp Physiol A* 182: 23–33
- Zill SN, Moran DT (1981a) The exoskeleton and insect proprioception. I. Responses of tibial campaniform sensilla to external and muscle-generated forces in the American cockroach, *Periplaneta americana*. *J Exp Biol* 91: 1–24
- Zill SN, Moran DT (1981b) The exoskeleton and insect proprioception. III. Activity of tibial campaniform sensilla during walking. *J Exp Biol* 94: 57–75
- Zill SN, Moran DT, Varela FC (1981) The exoskeleton and insect proprioception. II. Reflex effects of tibial campaniform sensilla. *J Exp Biol* 94: 43–55
- Zill SN, Fish SE, Frazier SF (1995) Knowing you have a leg to stand on: effects of trochanteral campaniform sensilla in cockroach walking. *Soc Neurosci Abstr* 21: 426